NEOPLASIA
www.neoplasia.com

Volume 20 Number 1 January 2018 pp. 44–56 44

FUS-CHOP Promotes Invasion in Myxoid Liposarcoma through a SRC/FAK/RHO/ROCK-Dependent Pathway[1]

Juan Tornin[*,†,2], Francisco Hermida-Prado[*,†,‡,2], Ranjit Singh Padda[§,¶], M. Victoria Gonzalez[‡,#], Carlos Alvarez-Fernandez[**], Veronica Rey[*,†], Lucia Martinez-Cruzado[*,†], Oscar Estupiñan[*,†], Sofia T. Menendez[*,†,‡], Lucia Fernandez-Nevado[*,†], Aurora Astudillo[††], Juan P. Rodrigo[*,†,‡], Fabrice Lucien[‡‡], Yohan Kim[§,¶,‡‡], Hon S. Leong[§,¶,‡‡], Juana Maria Garcia-Pedrero[*,†,‡] and Rene Rodriguez[*,†,‡]

*Hospital Universitario Central de Asturias-Instituto de Investigación Sanitaria del Principado de Asturias, Oviedo, Spain; [†]Instituto Universitario de Oncología del Principado de Asturias, Oviedo, Spain; [‡]CIBER de Cáncer (CIBERONC), Madrid, Spain; [§]Department of Pathology and Laboratory Medicine, Schulich School of Medicine and Dentistry, University of Western Ontario, London, ON, Canada; [¶]Translational Prostate Cancer Research Laboratory, Lawson Health Research Institute, London, ON, Canada; [#]Departamento de Cirugía, Universidad de Oviedo and Instituto Universitario de Oncología del Principado de Asturias, Oviedo, Spain; [**]Servicio de Oncología Médica, Hospital Universitario Central de Asturias, Oviedo, Spain; [††]Servicio de Anatomía Patológica, Hospital Universitario Central de Asturias, Oviedo, Spain; [‡‡]Department of Urology, Mayo Clinic, Rochester, MN

Abstract

Deregulated SRC/FAK signaling leads to enhanced migration and invasion in many types of tumors. In myxoid and round cell liposarcoma (MRCLS), an adipocytic tumor characterized by the expression of the fusion oncogene FUS-CHOP, SRC have been found as one of the most activated kinases. Here we used a cell-of-origin model of MRCLS and an MRCLS cell line to thoroughly characterize the mechanisms of cell invasion induced by FUS-CHOP using *in vitro* (3D spheroid invasion assays) and *in vivo* (chicken chorioallantoic membrane model) approaches. FUS-CHOP expression activated SRC-FAK signaling and increased the invasive ability of MRCLS cells. In addition, FAK expression was found to significantly correlate with tumor aggressiveness in sarcoma patient samples. The involvement of SRC/FAK activation in FUS-CHOP–mediated invasion was further confirmed using the SRC inhibitor dasatinib, the specific FAK inhibitor PF-573228, and FAK siRNA. Notably, dasatinib and PF573228 could also efficiently block the invasion of cancer stem cell subpopulations. Downstream of SRC/FAK signaling, we found that FUS-CHOP expression increases the levels of the RHO/ROCK downstream effector phospho-MLC2 (T18/S19)

Abbreviations: MRCLS, myxoid/round cell liposarcoma; FUS, fused in sarcoma; CHOP, C/EBP homologous protein; FAK, focal adhesion kinase; SFK, Src-family of protein kinases; RHO, RHOA/C GTPases; ROCK, Rho-associated coiled-coil-containing protein kinases 1 and 2; MLC2, myosin light chain 2; BMSC, bone marrow–derived mesechymal stem/stromal cell; FFPE, formalin-fixed, paraffin-embedded; CAM, chorioallantoic membrane; CSC, cancer stem cell.

Address all correspondence to: Rene Rodriguez, PhD, or Juana Maria Garcia-Pedrero, PhD, Laboratorio ORL-IUOPA, Hospital Universitario Central de Asturias-Instituto de Investigación Sanitaria del Principado de Asturias, Av. de Roma s/n, 33011 Oviedo, Spain.
E-mail: renerg.finba@gmail.com, rodriguezrene.uo@uniovi.es, juanagp.finba@gmail.com

[1] Author contributions: J. T. and F. H.-P.: development of methodology; performance of experimental procedures; acquisition, analysis, and interpretation of data. R. S. P, L. M.-C., O. E, S. T.-M., L. F.-N., and F.L.: performance of experimental procedures. M. V. G., C. A.-F., V. R., A. A., J. P. R., and H. S. L.: analysis and interpretation of data. J. M. G.-P. and R. R.: conception and design, analysis and interpretation of data, manuscript writing, and financial support. The manuscript has been seen and approved by all authors.

[2] These authors contributed equally to this work.

Received 18 August 2017; Revised 3 November 2017; Accepted 6 November 2017

1476-5586
https://doi.org/10.1016/j.neo.2017.11.004

and that this activation was prevented by dasatinib or PF573228. Moreover, the ROCK inhibitor RKI-1447 was able to completely abolish invasion in FUS-CHOP–expressing cells. These data uncover the involvement of SRC/FAK/RHO/ROCK signaling axis in FUS-CHOP–mediated invasion, thus providing a rationale for testing inhibitors of this pathway as potential novel antimetastatic agents for MRCLS treatment.

Neoplasia (2018) 20, 44–56

Introduction

Myxoid/round cell liposarcoma (MRCLS) is characterized by the recurrent translocations which fuse FUS (FUsed in Sarcoma; also termed TLS, Translocated in LipoSarcoma) or, less frequently, EWS to CHOP (C/EBP HOmologous Protein; also termed DDIT3, DNA Damage-Inducible Transcript 3). This type of liposarcoma shows a high tendency to recur locally or to metastasize to skeletal and pulmonary sites [1]. In addition, FUS-CHOP expression has been related with increased metastatic potential [2]. For MRCLS, treatment of metastatic disease mainly relies on cytotoxic drugs despite their limited clinical response [3]. Therefore, the study of the mechanisms involved in metastasis development may help to provide new therapeutic strategies to treat advanced and/or disseminated tumors more efficiently.

Nonreceptor protein tyrosine kinases, such as the focal adhesion kinase (FAK) and SRC proto-oncogene, are key signal transducers of a variety of cell surface receptors, including integrins and receptor tyrosine kinases [4–7]. Integrin stimulation induces FAK autophosphorylation at Y397, creating a high-affinity binding site for SRC. This association induces the autophosphorylation of SRC at Y419 and other conformational changes that lead full SRC activation [8]. Fully activated SRC can then further activate FAK by phosphorylation of its C-terminal domain (Y861 and Y925) and catalytic domain (Y576 and Y577) [5].

Deregulated activity of SRC-FAK signaling in cancer cells may lead to abnormal activation of several members of the Rho-family of GTPases, including RHOA/C (RHO) and RAC1, which are well-known regulators of cell migration and have been implicated in tumor cell invasion and metastasis [9,10]. In addition, the concurrent activation of signaling pathways like those mediated by PI3K-AKT, ERK, or JNK may induce prosurvival signals and the upregulation of proteolytic proteins that may contribute to the invasion process [4,5,9,11–15].

Tumor cells have been observed to migrate and invade as single cells, as loosely attached cell streams, or as compact and cohesive collectives by activating the above-mentioned signaling pathways. The type of cell migration is determined by both intrinsic and microenvironmental factors, such as the cell morphology, the degree of cell-cell adhesion, the existing supracellular signaling, and the physical properties of the microenvironment [12,16,17]. In the collective migration modes, one or several leader cells extend protrusions that generate traction forces and may induce proteolysis of the surrounding matrix. As a consequence, following cells are passively dragged behind along the migration track by cell-cell adhesion forming cell streams, small clusters, or well-organized masses [12,16,17]. During the invasion process, cells may switch from a collective to an individual mode of invasion. This transition occurs when the cell-cell and cell-extracellular matrix interactions are weakened and is influenced by several physical and molecular cues [12,18]. According to the type of cell movement, two main models of individual cell invasion with different requirements for Rho GTPs and proteolytic proteins have been described [9,12,14,19,20]. The "elongated-mesenchymal" mode is characterized by the formation of actin-rich protrusions at the front of the cell and is mainly driven by the activation of RAC1-induced signaling. The "rounded-amoeboid" movement is supported by high levels of actomyosin contractility which is induced by RHO-induced signaling. Thus, RHO activates the Rho-associated coiled-coil–containing protein kinases 1 and 2 (ROCK) resulting in the accumulation of the phosphorylated form of myosin light chain 2 (MLC2) at S19 which promotes actomyosin contractility [12]. Although better described for individual cell invasion models, mesenchymal and amoeboid morphologies and their associated signaling are also observed in collective cell invasion models [21].

In accordance with the protumorigenic role of altered SRC/FAK signaling or Rho GPase activity, these factors have been frequently found to be overexpressed in different tumor types and correlated with poor prognosis and increased invasive and metastatic potential [9,22–25]. Therefore, the clinical efficacy of several inhibitors with proved activity on SRC, like dasatinib, FAK, or ROCK, is being tested in many other solid tumors [7,26,27].

In sarcoma, several studies reported an increased activation of SRC in patient samples and cell lines derived from different sarcoma subtypes [28,29]. Furthermore, the inhibition of this activity with dasatinib reduced tumor cell growth and migration in liposarcoma, including myxoid liposarcoma, synovial sarcoma, and bone sarcoma cell lines [28–30]. Likewise, the expression and activation status of FAK have been related with decreased overall survival and metastasis-free survival and increased migration in osteosarcoma [31]. In addition, FAK inhibition resulted in decreased invasion, migration, and tumor growth in rhabdomyosarcoma [32]. Here, we used our previously developed MRCLS model [33,34], as well as an MRCLS cell line, to thoroughly characterize the mechanisms used by FUS-CHOP to promote cell invasion. Using both *in vitro* and *in vivo* approaches, we found that FUS-CHOP–induced invasive properties are mediated through the activation of SRC/FAK/RHO/ROCK signaling. These findings provide a rationale for testing inhibitors of this route as a novel therapeutic strategy for MRCLS.

Materials and Methods

Cell Types, Drugs, and Ethics Statement

Human BM-MSCs sequentially mutated with up to five oncogenic events were generated, characterized, and cultured as previously

described (Supplemental Information; Table S1) [33–35]. The myxoid liposarcoma cell line 1765-92 was donated by Dr. R Mantovani (Università degli Studi di Milano, Italy). Tumorsphere formation protocol was previously described [36]. Dasatinib, PF-573228, BYL-719, and RKI-1447 were obtained from Selleckchem, (Houston, TX) (supplemental information). All experimental protocols have been performed in accordance with institutional review board guidelines and were approved by the Institutional Ethics Committee of the Hospital Universitario Central de Asturias. All samples from human origin were obtained upon signed informed consent.

Western Blotting

Whole cell protein extraction and Western blot analysis were performed as previously described [36]. Antibodies used are described in Supplemental Information. Quantification of the protein bands (IRDye fluorescent signals) was performed using the Odyssey Fc imaging system and the software Image Studio from LICOR (Lincoln, NE).

Three-Dimensional Spheroid Invasion Assays

Cells were suspended in DMEM plus 5% methyl cellulose (Sigma) at 80,000 cells/ml to form cell spheroids (2000 cells/spheroid) by serial pipetting of 25 µl into a nonadhesive Petri dish, and incubated in an inverted position for 18 hours. Next day, each cell spheroid was transferred to an individual well of 96-well plate and embedded into a volume of 70 µl of 3 mg/ml bovine collagen type I matrix (PureCol) from Advanced Biomatrix (San Diego, CA) and filled with 100 µl of complete media. Collective cell invasion was monitored using a Zeiss Cell Observer Live Imaging microscope (Zeiss, Thornwood, NY) coupled with a CO_2 and temperature-maintenance system. Time-lapse images were acquired every 15 minutes during 24 hours using a Zeiss AxioCam MRc camera. The invasive area was determined by calculating the difference between the final area (t = 24 hours) and the initial area (t = 0 hour) using image J analysis program, and data were normalized to the control cells. Three independent experiments including four replicates for each condition were performed.

Cell Viability Assays

The viability of all cell lines in the presence and absence of drugs was determined using the cell proliferation reagent WST-1 (Roche, Mannheim, Germany) as described before [36]. Three independent experiments were performed including triplicates for each condition. As previously reported, no significant differences were found in the doubling times of the cell types analyzed [35].

siRNA and shRNA

A pool of FAK-specific siRNAs (On-Target plus PTK-2 siRNA, L-003164-00-0005) and a siGenome RiSC-Free control siRNA (siControl; D-001220-01) were from Dharmacon (Lafayette, CO). Cells were transfected with 100 pmol/ml siRNAs using Lipofectamine 3000 (Thermo Fisher) as described [36]. MSC-4H-FC cells depleted of FUS-CHOP expression were generated by transduction with lentiviral particles carrying a CHOP-shRNA expression vector (TRCN0000368983) from Sigma (St. Louis, MO) as previously described [33].

Patients and Immunohistochemical Analysis

The clinicopathologic features of the 82 sarcoma samples and patients treated at the Hospital Universitario Central de Asturias and their tumors are included in Table S2. Tumor grade was evaluated in H&E-stained preparations using the French Federation of Comprehensive Cancer Centers grading system [37] (further details in Supplemental Materials and Methods). Tissue microarrays were prepared with retrospectively collected tissue specimens (FFPE), and immunohistochemical analysis of FAK expression was performed as detailed in the Supplemental Materials and Methods section [24]. The immunostaining showed a homogeneous distribution and was scored blinded to clinical data by two independent observers as low or high protein expression levels. The experimental results distributed among the different clinical groups of tumors were tested for significance employing the χ^2 test (with Yates' correction, when appropriate). The statistical analysis was carried out with the software package SPSS 19.0 (SPSS, Inc., Chicago, IL). All tests were two-sided, and values of $P < .05$ were considered statistically significant.

Cell Extravasation Assay Using Chick Chorioallantoic Membrane (CAM) Model

Day 13 chick embryos were used for cell extravasation assay as described earlier [38]. Four to 10 chick embryos were injected for each condition, and the percentage of extravasated cells in three different regions of each embryo was calculated. For intravascular cell imaging, the chick embryos were injected with lectin and dextran to label the CAM vessel walls and lumen, respectively. At t = 24 hours post intravenous injection of cells, intravital images of extravasated cancer cells were obtained *via* confocal microscopy as described [38].

Results

FUS-CHOP Expression Activates SRC-FAK Signaling and Increases the Invasive Potential

To study the ability of FUS-CHOP to alter cell signaling in sarcoma-initiating cells, we used previously developed models in which this fusion oncogene (MSC-4H-FC cells) or the corresponding control vector (MSC-4H-GFP cells) was expressed in human bone marrow MSCs (BM-MSCs), the cell-of-origin for different types of sarcomas [39,40], pretransformed with four oncogenic events (Table S1) [34]. Opposite to MSC-4H-GFP, MSC-4H-FC cells were fully transformed and able to generate MRCLS *in vivo* [33].

Previous works have found that SRC signaling is one of the most active pathways in MRCLS [29,41]. Then, we used our MRCLS model to study whether the expression of FUS-CHOP is directly responsible of the activation of SRC and its signaling partner FAK. We found that, compared to MSC-4H-GFP cells, FUS-CHOP expression in MSC-4H-FC cells increased the phosphorylation levels of activating residues in SRC (Y-419) and FAK (Y-397) as well as the total protein levels of FAK (Figure 1*A* and Supplementary Figure S1). The ratio between phospho-FAK (Y-397) levels and total FAK protein showed no relevant changes in MSC-4H-GFP and MSC-4H-FC cells, indicating that the increase of the phosphorylated form of FAK induced by FUS-CHOP is mainly due to an upregulation of the total form of FAK rather than by an overactivation of the mechanisms leading to the phosphorylation of FAK (Figure S1*B*). Confirming the ability of FUS-CHOP to activate this pathway, its depletion in MSC-4H-FC cells using an shRNA designed to target CHOP prevented SRC/FAK activation, thereby reducing the levels of phospho-SRC (Y-419), phospho-FAK (Y-397), and total FAK (Figure 1*A* and Supplementary Figure S1).

Given the suggested role of activated SRC and/or FAK in invasion [4,5,9], we next analyzed whether FUS-CHOP–expressing

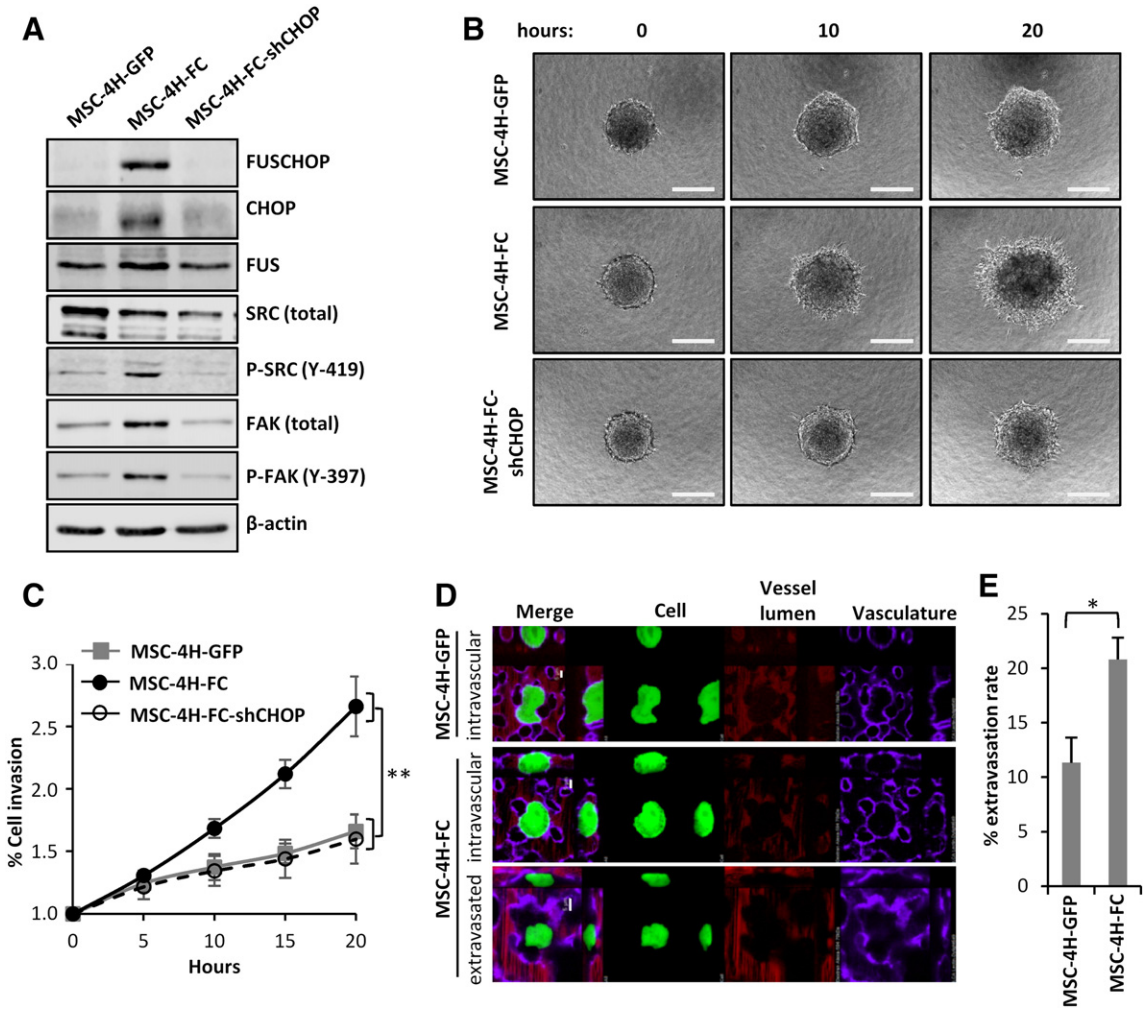

Figure 1. FUS-CHOP expression activates SRC/FAK signaling and increases invasive properties. (A) Western blotting analysis of the indicated proteins in MSC-4H-GFP, MSC-4H-FC, and MSC-4H-FC cells depleted for FUS-CHOP expression using CHOP shRNA (MSC-4H-FC-shCHOP cells). β-Actin levels were used as loading control. Quantification of three independent experiments is plotted in Supplementary Figure S1. (B and C) Analysis of the invasive properties of MSC-4H-GFP, MSC-4H-FC, and MSC-4H-FC-shCHOP cells using 3D spheroid invasion assays. Representative images of the 3D invading spheroids at the indicated times of assay (B) and quantification of the invasive area (C) are presented. Scale bars = 200 μm. (D) Representative 3D volume confocal images (60× magnification) of MSC-4H-GFP, MSC-4H-FC cells in the intravascular space (top and middle panels, respectively), and a representative extravasated MSC-4H-FC cell (bottom panel) post intravenous injection into the chicken embryo CAM vasculature. GFP-positive cells (green), CAM vasculature labeled using lectin-Dylight649 (violet), and CAM vessel lumen using dextran (red) are shown. Scale bar = 5 μm. (E) Quantification of extravasation efficiency of MSC-4H-GFP and MSC-4H-FC cell lines 24 hours postinjection. Error bars represent the standard deviation (SD), and asterisks indicate statistically significant differences with respect to the MSC-4H-FC values (*: $P < .05$; **: $P < .01$; two-sided Student t test).

MRCLS-forming cells showed increased invasive properties. With this purpose, we studied the ability of MRCLS spheroids to invade 3D collagen matrices, an invasion assay that takes into account both cell-cell contact between adjacent tumor cells and the need for a 3D supporting matrix [42]. Using live cell time-lapse microscopy, we found that MSC-4H-FC spheroids showed highly increased invasive properties when compared with MSC-4H-GFP spheroids. Importantly, these statistically significant differences were completely reverted by FUS-CHOP depletion in MSC-4H-FC-shCHOP spheroids (Figure 1, *B* and *C* and Videos S1-S3).

To validate these findings *in vivo,* we evaluated invasiveness phenotypes by quantifying the rates of cancer cell extravasation in the chorioallantoic membrane (CAM) of chicken embryos [38]. MSC-4H-GFP and MSC-4H-FC cells were intravenously injected into the vasculature of day 13 chicken embryos followed by assessment of extravasation efficiency 24 hours postinjection. We observed that both cell types were able to extravasate out of the CAM vasculature; however, in accordance with *in vitro* results, MSC-4H-FC cells showed a significant increase in the extravasation efficiency (Figure 1, *D* and *E*).

Inhibition of SRC or FAK Activation Prevents the Invasion of FUS-CHOP–Expressing Cells

To study whether the activation of SRC plays a role in the increased invasive properties of MSC-4H-FC cells, we treated these cells with dasatinib. A 24-hour treatment with low micromolar concentrations of dasatinib efficiently inhibited SRC (Y419) phosphorylations without affecting total protein levels of SRC

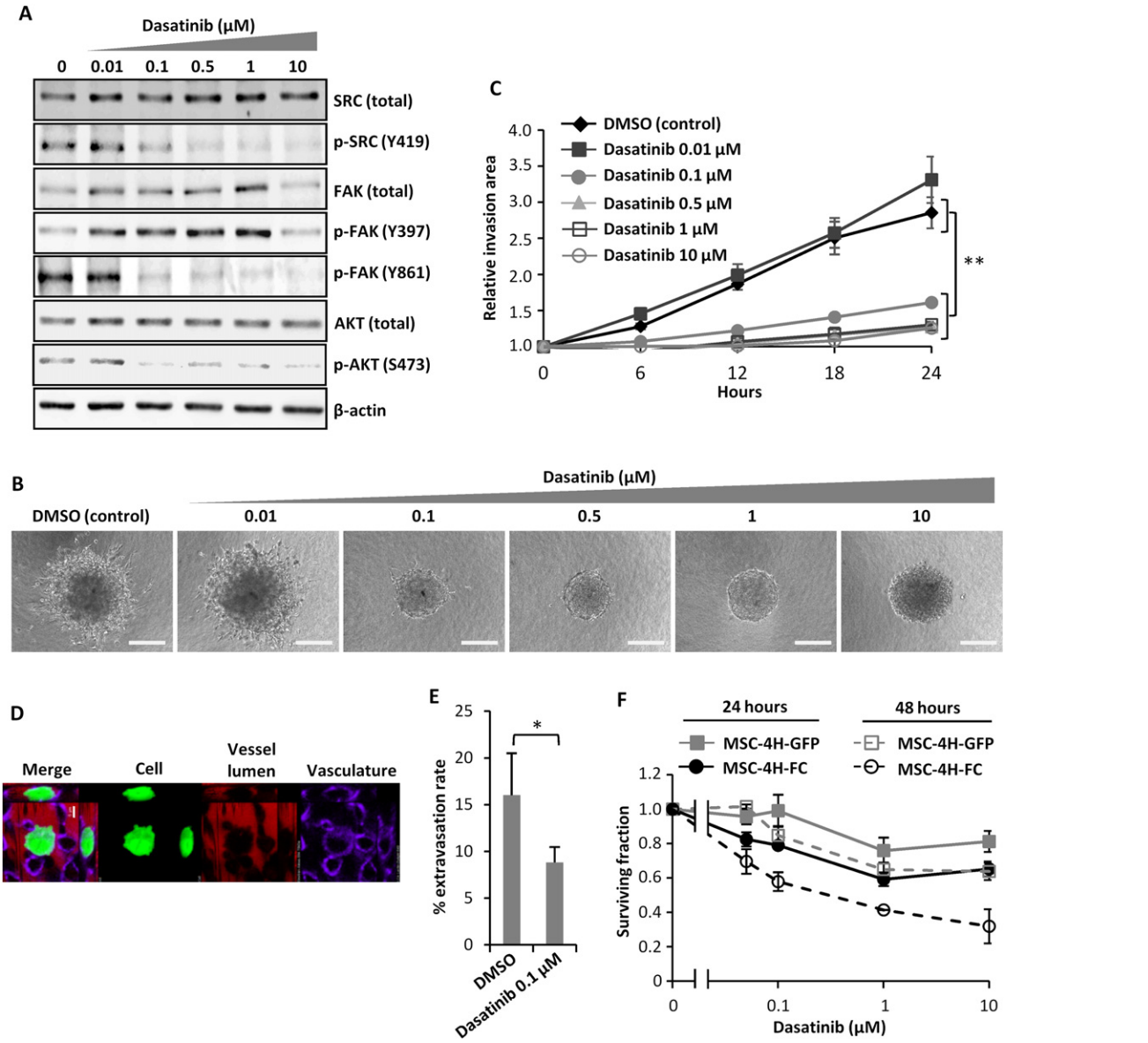

Figure 2. Inhibition of SRC prevents the invasion of FUS-CHOP–expressing cells. (A) Western blotting analysis of the indicated proteins in MSC-4H-FC cells treated with increasing concentrations of dasatinib for 24 hours. β-Actin levels were used as loading control. Quantification of three independent experiments is plotted in Supplementary Fig S2. (B and C) Effect of increasing concentrations of dasatinib on the invasive properties of MSC-4H-FC cells using 3D spheroid invasion assays. Representative images of the 3D spheroids treated with the indicated concentrations of dasatinib for 24 hours (B) and quantification of the invasive area (C) are presented. Scale bars = 200 μm. (D) Representative 3D volume confocal image (60× magnification) of MSC-4H-FC cells pretreated with 0.1 μM dasatinib for 24 hours followed by intravenous injection into the chicken embryo CAM vasculature. GFP-positive cells (green), CAM vasculature labeled using lectin-Dylight649 (violet), and CAM vessel lumen using dextran (red) are shown. Scale bars = 5 μm. (E) Quantification of extravasation efficiency of control and dasatinib-treated MSC-4H-FC cells 24 hours postinjection. (F) Cell viability (WST1 assay) measured after the treatment of the indicated cell lines with increasing concentrations of dasatinib for 24 or 48 hours. Error bars represent the SD, and asterisks indicate statistically significant differences with respect to the control values (*: $P < .05$; **: $P < .01$; one-sided Student t test).

(Figure 2*A* and Supplementary Figure S2). In the case of FAK, low concentrations of dasatinib induced an increase in total FAK levels and its autophosphorylated form [FAK (Y397)], which is not observed with higher drug concentrations. In any case, dasatinib efficiently inhibited SRC-dependent phosphorylation of FAK on Y861, which is a requisite for an effective activation of this kinase (Figure 2*A* and Supplementary Figure S2) [5]. In addition, the phosphorylation/activation of AKT (S473) was also reduced upon dasatinib treatment as efficiently as phospho-SRC (Y419) or phospho-FAK (Y861) (Figure 2*A* and Supplementary Figure S2). Furthermore, concentrations of dasatinib as low as 0.1 μM completely abolished the invasion of MSC-4H-FC spheroids into 3D collagen matrices (Figure 2, *B* and *C* and Videos S4-S9). Similarly, 0.1 μM of dasatinib was able to significantly inhibit cell extravasation in the *in vivo* CAM model (Figure 2, *D* and *E*). This potent anti-invasive effect of dasatinib cannot be attributed to the antiproliferative properties since 24-hour treatment with low dasatinib doses only produced a mild cytotoxic effect. Even the higher assayed concentrations (10 μM) led to

surviving fractions of 80% and 65% for MSC-4H-GFP and MSC-4H-FC cells, respectively (Figure 2*F*). Nonetheless, these surviving fractions decreased to 65% and 40% after 48-hour treatment with this inhibitor (Figure 2*F*).

We next studied the effect of FAK inhibition using the specific inhibitor PF-573228. A 24-hour treatment with PF-573228 caused an effective dose-dependent inhibition of FAK phosphorylation (Figure 3*A* and Supplementary Figure S3, *A* and *B*). In addition, phospho-AKT (S473) was completely inhibited at the higher concentration assayed (10 μM). On the other hand, phospho-SRC (Y419) was unaffected after the treatment. Mimicking the inhibitory effect on FAK phosphorylation, PF-573228 induced a dose-dependent inhibition of the invasive capability of MSC-4H-FC spheroids (Figure 3, *B* and *C* and Videos S10-S14). *In vivo*, 10 μM of PF-573228 also inhibited cell extravasation out of the CAM vasculature (Figure 3, *D* and *E*). Interestingly, intravital imaging revealed the release of extracellular vesicles or microparticles by intravascular PF-573228–treated cells into the stroma [43] (Figure 3*D*). Similar to that observed for dasatinib, 24-hour treatment with PF-573228 only induced mild/moderate antiproliferative effects in MSC-4H-GFP and MSC-4H-FC cells, although cytotoxicity increased at 48-hour treatment (Figure 3*F*).

To further confirm the role of FAK in the invasive properties of FUS-CHOP–expressing MRCLS-initiating cells, we performed siRNA-mediated depletion of this kinase in MSC-4H-FC cells. Western blotting analysis confirmed an efficient knockdown of both the total and phosphorylated forms of FAK (Figure 3*G* and Supplementary Figure S3*C*). Similar to that observed by pharmacologic inhibition of FAK, phospho-AKT (S473) levels also decreased upon FAK depletion, while SRC (Y-419) phosphorylation, instead of being reduced, was increased (Figure 3*G* and Supplementary Figure S3*C*). In 3D invasion assays, we found that MSC-4H-FC spheroids generated using FAK-depleted cells were completely unable to invade collagen matrices (Figure 3, *H* and *I* and Videos S10-S16), thus confirming the critical role of FAK in FUS-CHOP–mediated invasion.

As seen, phosphorylation/activation of AKT (S473) was efficiently downregulated by dasatinib (Figure 2*A*), PF-573228 (Figure 3*A*), or FAK-siRNA (Figure 3*E*). To investigate a possible role of PI3K/AKT signaling as a downstream effector of SRC/FAK proinvasive signals, we treated MSC-4H-FC cells with the PI3K inhibitors BYL-719. At a concentration that prevented AKT phosphorylation (Figure S4*A*), this inhibitor was not able to inhibit 3D spheroid invasion (Figure S4*B*), thus suggesting that SRC/FAK proinvasive signals do not require the activation of PI3K/AKT pathway.

Finally, we aimed to test whether the SRC/FAK inhibition could also affect invasiveness using another MRCLS model. Therefore, we treated the 1765-92 cell line with dasatinib or PF-573228 and checked phospho-SRC and phospho-FAK levels as well as the ability to invade. Consistent with our results in MSC-4H-FC cells, dasatinib inhibited the phosphorylation of SRC (Y419) and AKT (S473), while PF-573228 efficiently reduced the phosphorylation levels of FAK (Y397) and AKT (S473) but not SRC (Y419) (Figure 4*A* and Supplementary Figure S5). Accordingly, both inhibitors also efficiently prevented the 3D invasive capability of this MRCLS cell line (Figure 4, *B* and *D* and Videos S17-S20), without significantly affecting its proliferation rate (Figure 4*E*).

Altogether, these results suggest that the activation of the SRC/FAK-mediated signaling is essential to maintain the invasive properties of FUS-CHOP–expressing MRCLS cells, and clearly demonstrate that SRC/FAK inhibition may represent an effective anti-invasive therapeutic strategy.

FAK Expression Correlates with Tumor Aggressiveness in Sarcoma Tissue Specimens

Next, we aimed to investigate whether enhanced expression of FAK in sarcoma patients is clinically relevant. To this purpose, we generated tissue microarrays including FFPE samples from 66 malignant sarcomas and 16 benign/low-malignant sarcoma-related lesions (Table 1 and Supplementary Table S2), and FAK expression was analyzed by immunohistochemistry (Figure 5). High levels of FAK expression were observed in 48.5% (32/66) of malignant sarcomas. Importantly, high levels of FAK significantly correlated with tumor grade (P = .004). Interestingly, when FAK expression was compared between malignant and benign/low-malignant tumors, high FAK expression was strongly and significantly associated with malignant sarcomas (P = .009). Finally, although the number of liposarcomas included in this series was relatively low (10 MRCLS and 8 liposarcomas of other subtypes), a tendency was observed for higher expression levels of FAK in MRCLS compared to other liposarcoma subtypes (P = .09) (Figure 5, Table 1, and Supplementary Table S2). These results are in line with the tight association between FUS-CHOP and FAK expression/activity observed in our MRCLS model.

Inhibition of SRC or FAK Prevents the Invasion of Cancer Stem Cell (CSC)–Enriched Subpopulations

CSC subpopulations are thought to be responsible for tumor invasion and metastatic dissemination [39]. We previously showed that sarcoma models originated from transformed MSCs were able to grow as floating tumorspheres with enhanced CSC properties [44]. Therefore, we studied whether the inhibition of SRC or FAK could also be an effective strategy to inhibit the invasive potential of these subpopulations (Figure 6*A*). First, we found that tumorsphere cultures of MSC-4H-GFP cells showed higher levels of phospho-FAK (Y861 and Y397), phospho-SRC (Y418), and phospho-AKT (S473) than unselected adherent cultures, while the levels of these phospho-kinases remained consistently high in MSC-4H-FC adherent and tumorsphere cultures (Figure 6*B* and Supplementary Figure S6). As expected, we found that spheroids formed from MSC-4H-FC tumorspheres were able to invade 3D collagen matrices more efficiently than spheroids derived from the fraction of cells unable to form tumorspheres (Figure 6, *C* and *D* and Videos S21-S24). Notably, dasatinib and PF-573228 were able to reduce invasion in spheroids-derived from tumorspheres (Figure 6, *C* and *D* and Videos S22-S24) as efficiently as in those derived from the unselected bulk tumor population (Figure 2*C* and Supplementary Figure 3*C*).

Altogether, these results indicate that FAK inhibition prevents self-renewal and invasive potential of FUS-CHOP–expressing CSCs.

FUS-CHOP–Induced Invasion is Mediated through a RHO/ROCK-Dependent Mechanism

Based on transcriptomics analysis, we previously found that the RHO family of GTPases was among the signaling pathways most significantly altered by FUS-CHOP expression in hMSCs [33]. Given the predominant role of certain members of this family in tumor invasion, we wondered whether RHO/ROCK signaling could be involved in SRC/FAK-mediated invasion induced by FUS-CHOP.

First, we found that FUS-CHOP–expressing cells showed increased levels of the RHO/ROCK downstream effector MLC2 and its active phosphorylated form MLC2 (T18/S19) (Figure 7*A* and Supplementary Figure S7, *A* and *B*). The ratio between phosphorylated and total forms of MLC2 was 3 times higher in MSC-4H-FC than in MSC-4H-GFP (Figure S7*B*), indicating that FUS-CHOP expression may act by regulating both the phosphorylation levels and the total MLC2 protein expression. This accumulation of phospho-MLC2 in MSC-4H-FC cells was efficiently inhibited by increasing doses of the ROCK specific inhibitor RKI-1447 [45] (Figure 7*B* and Supplementary Figure S7, *C* and *D*). Importantly, concentrations of RKI-1447 as low as 0.5 μM were able to completely abolish the invasion of MSC-4H-FC 3D spheroids (Figure 7*C* and *D* and Videos S25-S29) and to significantly reduce cell extravasation out of the CAM vasculature (Figure 7*E*) without having any relevant effect on cell proliferation (Figure 7*F*). These

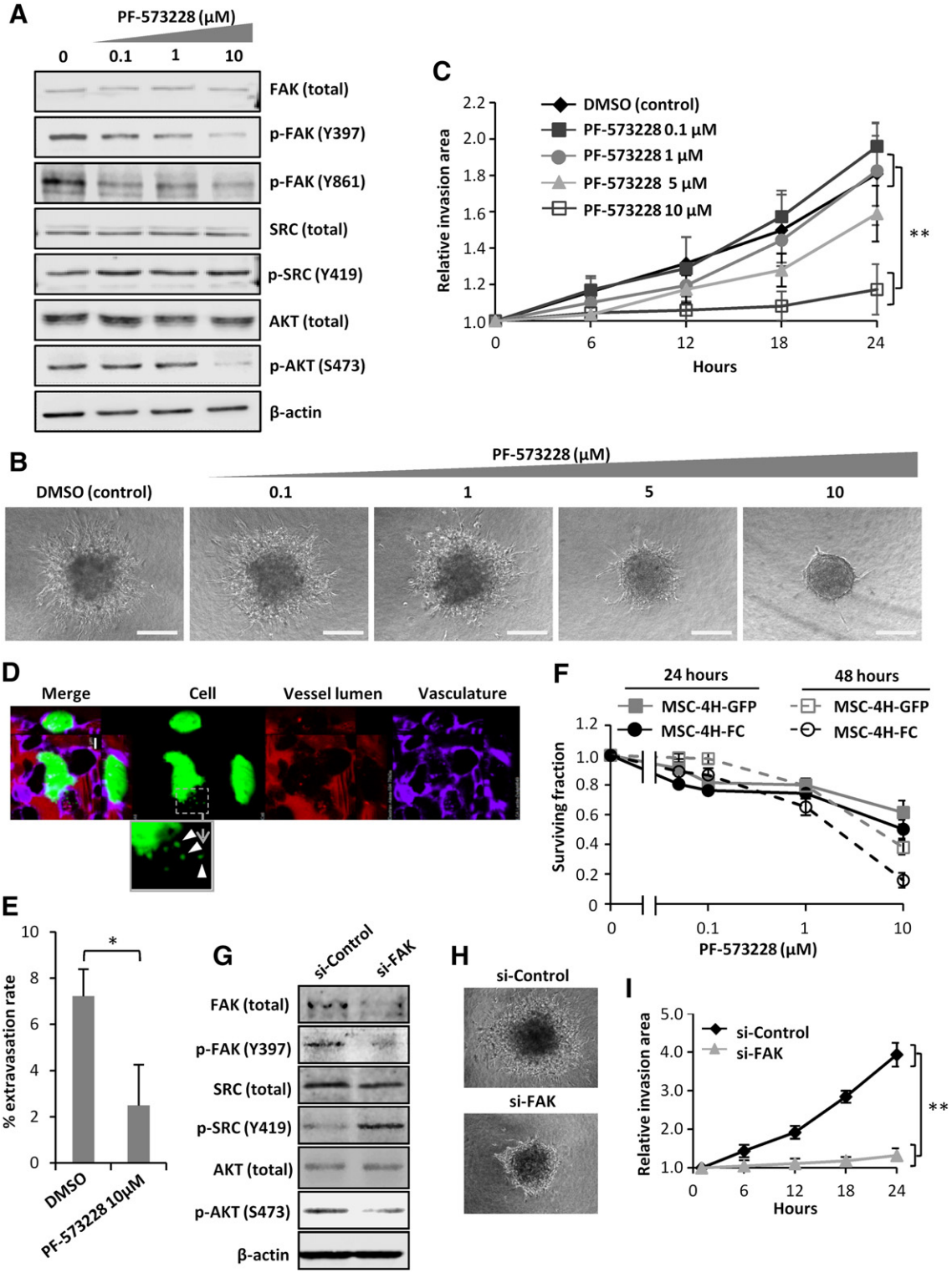

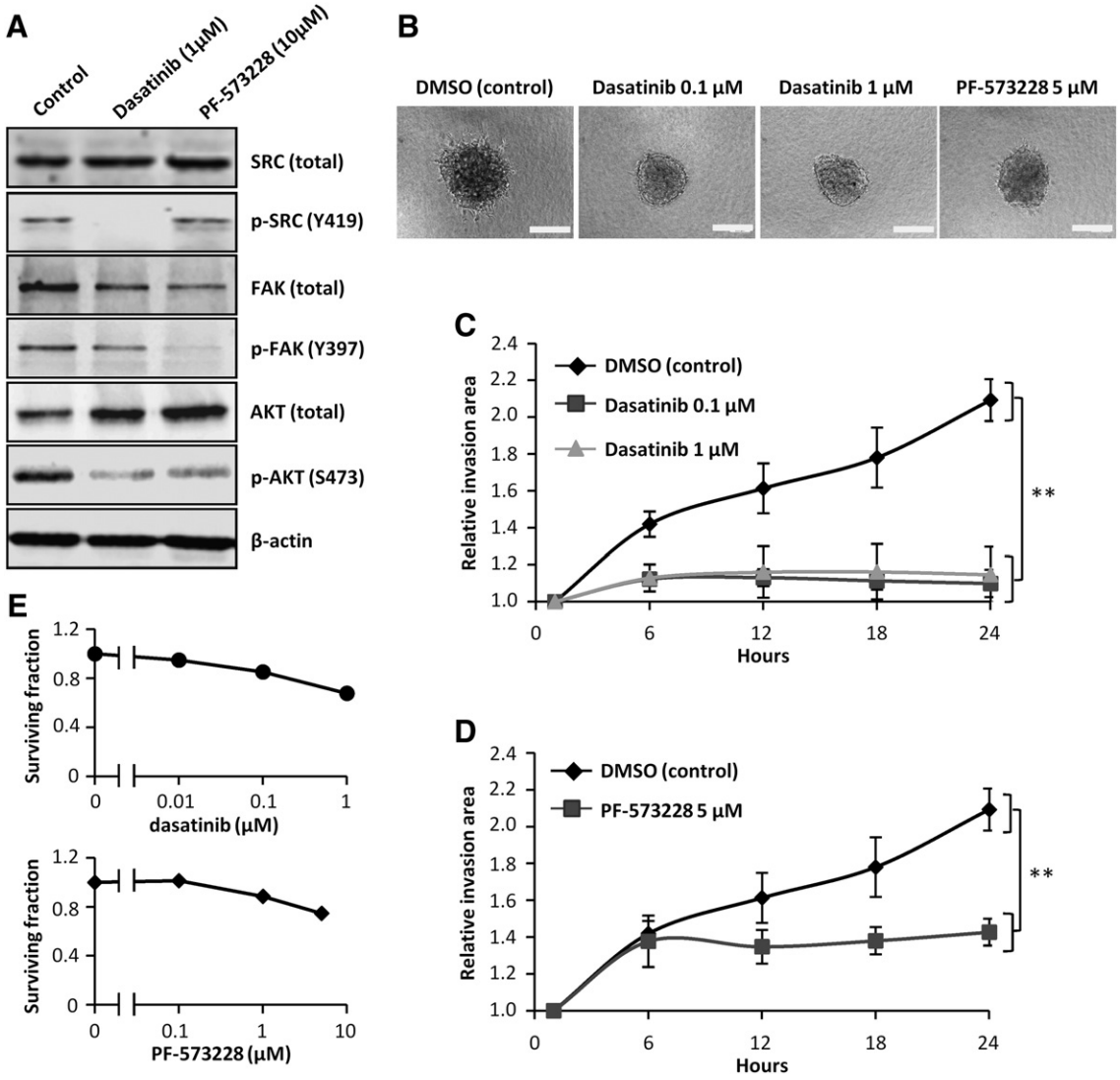

Figure 4. Inhibition of SRC or FAK prevents the invasion of the MRCLS cell line 1765-92. (A) Western blotting analysis of the indicated proteins in 1765-92 cells treated with 1 μM dasatinib or 10 μM PF-573228 for 24 hours. β-Actin levels were used as loading control. Quantification of three independent experiments is plotted in Supplementary Fig S5. (B and D) Analysis of the effect of dasatinib and PF-573228 in the invasive properties of 1765-92 cells using 3D spheroid invasion assays. Representative images of the 3D invading spheroids treated with the indicated inhibitors for 24 hours (B) and quantification of the invasive area of cells treated with dasatinib (C) and PF-573228 (D) are presented. Scale bars = 200 μm. (E) Cell viability (WST1 assay) measured after treatment of 1765-92 cells with increasing concentrations of dasatinib (top panel) or PF-573228 (bottom panel) for 24 hours. Error bars represent the SD, and asterisks indicate statistically significant differences with the control series (*: $P < .05$; **: $P < .01$; one-sided Student t test).

Figure 3. Inhibition of FAK prevents the invasion of FUS-CHOP–expressing cells. (A) Western blotting analysis of the indicated proteins in MSC-4H-FC cells treated with increasing concentrations of PF-573228 for 24 hours. β-Actin levels were used as loading control. Quantification of three independent experiments is plotted in Supplementary Fig S3. (B and C) Analysis of the effect of increasing concentrations of PF-573228 on the invasive properties of MSC-4H-FC cells using 3D spheroid invasion assays. Representative images of the 3D spheroids treated with the indicated concentrations of PF-573228 for 24 hours (B) and quantification of the invasive area (C) are presented. Scale bars = 200 μm. (D) Representative 3D volume confocal image (60× magnification) of MSC-4H-FC cells pretreated with 10 μM PF-573228 for 24 hours followed by intravenous injection into the chicken embryo CAM vasculature. GFP-positive cells (green), CAM vasculature labeled using lectin-Dylight649 (violet), and CAM vessel lumen using dextran (red) are shown. The release of extracellular vesicles/microparticles is indicated in the enlarged area. Scale bars = 5 μm. (E) Quantification of extravasation efficiency of control and PF-573228-treated MSC-4H-FC cells 24 hours postinjection. (F) Cell viability (WST1 assay) measured after treatment of the indicated cell lines with increasing concentrations of PF-573228 for 24 or 48 hours. (G) Protein levels of the indicated proteins in MSC-4H-FC cells transfected with the indicated siRNAs. Quantification is plotted in Supplementary Fig S3. (H and I) Effect of FAK depletion by siRNA on the invasive properties of MSC-4H-FC cells. Representative images of the 3D invading spheroids after 24 hours (H) and quantification of the invasive area (I) are presented. Error bars represent the SD, and asterisks indicate statistically significant differences with the control series (*: $P < .05$; **: $P < .01$; one-sided Student t test).

Table 1. Distribution of Malignant (N = 66) and Benign (N = 16) Sarcoma Cases According to Their FAK Expression Level Across Categories of the Indicated Patient Characteristics and Tumor Clinicopathologic Parameters (a More Comprehensive Description is Presented as Table S2). *P* Values are Shown

	Low FAK (%)	High FAK (%)	Total (%)	*P* (Chi-Square)
Malignant cases	34 (51.5)	32 (48.5)	66	
Tumor type				
Osteosarcoma	4 (11.8)	4 (12.5)	8 (12.1)	.047
Ewing sarcoma	2 (5.9)	3 (9.4)	5 (7.6)	
Myxoid liposarcoma	7 (20.6)	3 (9.4)	10 (15.2)	
Liposarcoma (other subtypes)	8 (23.5)	0 (0)	8 (12.1)	
Chondrosarcoma	6 (17.6)	5 (15.6)	11 (16.7)	
Synovial sarcoma	3 (8.8)	6 (18.8)	9 (13.6)	
Pleomorphic sarcoma	4 (8.8)	7 (21.9)	10 (15.2)	
GIST	1 (2.9)	4 (12.5)	5 (7.6)	
Total	34	32	66	
Tumor grade				
1	13 (46.4)	1 (4.4)	14 (27.4)	.004
2	8 (28.6)	10 (47.8)	19 (37.3)	
3	7 (25)	11 (47.8)	18 (35.3)	
Total	28	23	51	
Missing	6	9	15	
Myxoid liposarcoma *vs* liposarcoma (other subtypes)				
Myxoid liposarcoma	7 (46.7)	3 (100)	10 (55.6)	.09
Liposarcoma (other subtypes)	8 (53.3)	0	8 (44.4)	
Total	15	3	18	
Benign cases	14 (87.5)	2 (12.5)	16	
Tumor type				
Encondroma	7 (50.0)	0 (0)	7 (43.75)	.182
Dermatofibrosarcoma	7 (50.0)	2 (100)	9 (56.35)	
Total	14	2	16	
Malignant *vs* benign tumors				
Benign	14 (29.2)	2 (5.9)	16 (19.5)	.009
Malignant	34 (70.8)	32 (94.1)	66 (80.5)	
Total	48	34	82	

data indicate that the activation of RHO/ROCK signaling leading to the phosphorylation of MLC2 is essential to maintain the invasive properties of FUS-CHOP–expressing cells. In addition, both dasatinib and PF-573228 were able to prevent MLC2 phosphorylation (Figure 7*B* and Supplementary Figure S7, *C* and *D*), thus reflecting that SRC and FAK are upstream mediators of the activation of RHO/ROCK signaling.

Altogether, these results indicate that FUS-CHOP–expressing cells may invade through a mechanism involving the activation of the SRC/FAK/RHO/ROCK signaling axis.

Discussion

Deregulated SRC/FAK signaling has been extensively related with enhanced migration and invasion in many types of tumors [5,9]. In MRCLS, SRC is one of the kinases more frequently activated in both primary and established cell lines, as well as in patient samples, and SRC inhibition with dasatinib reduced their migratory and invasive potential [29,30,41]. In addition, the expression of FUS-CHOP in sarcoma cell lines increases migration and invasion and enhances the metastatic potential in these cells [2]. Altogether, these reports suggest that FUS-CHOP might promote proinvasive phenotypes in MRCLS through SRC-mediated signaling. Therefore, we studied the contribution of SRC activation and that of its signaling partner FAK to sarcoma invasion by using our previously described MRCLS model, in which FUS-CHOP expression in pretransformed hBMSCs is able to drive MRCLS formation *in vivo* [33]. To deeply characterize the mechanisms involved in FUS-CHOP–induced invasion, we used 3D collagen matrices which are reported to closely mimic the fibrillar collagen meshworks present in most connective tissues [46] and therefore represent a relevant *in vitro* model to reproduce the microenvironment of many sarcomas. In addition, we also quantified

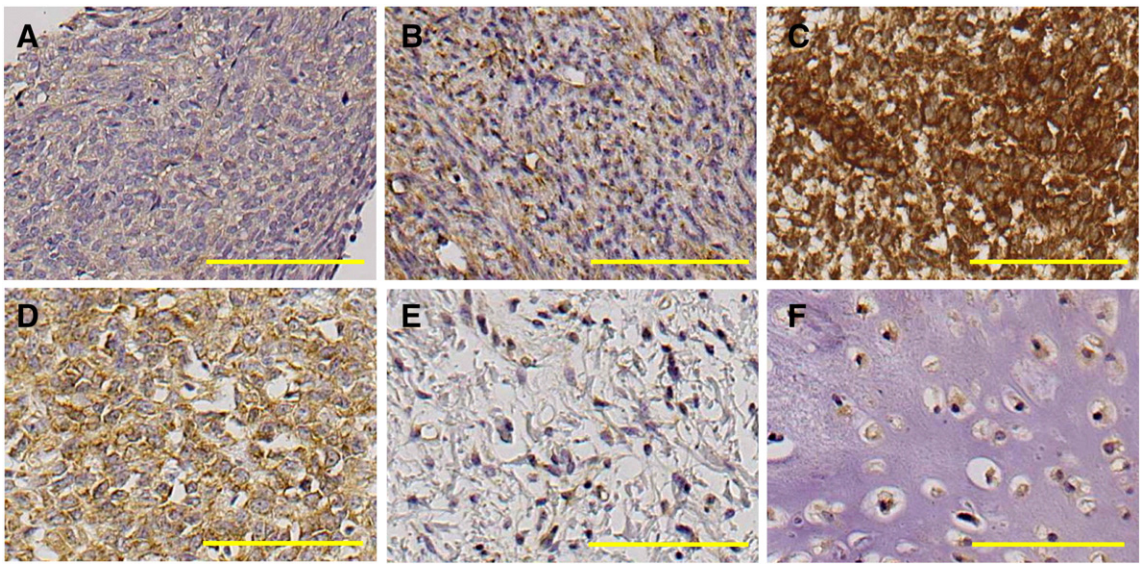

Figure 5. Immunohistochemical analysis of FAK expression in sarcoma samples. Representative images showing different levels of cytoplasmic FAK staining in sarcoma samples. (A-C) Synovial sarcoma samples showing a correlation of FAK expression with tumor grade (A: low FAK–grade 1 tumor; B: low FAK–grade 2 tumor; C: high FAK–grade 3 tumor). (D and E) MRCLS samples tend to show higher levels of FAK expression than other liposarcoma subtypes (D: high FAK–grade 2 MRCLS; E: low FAK–grade 1 well-differentiated spindle cell liposarcoma). (F) Encondroma sample representing that most benign tumor samples displayed low levels of FAK expression. Scale bar = 100 μm.

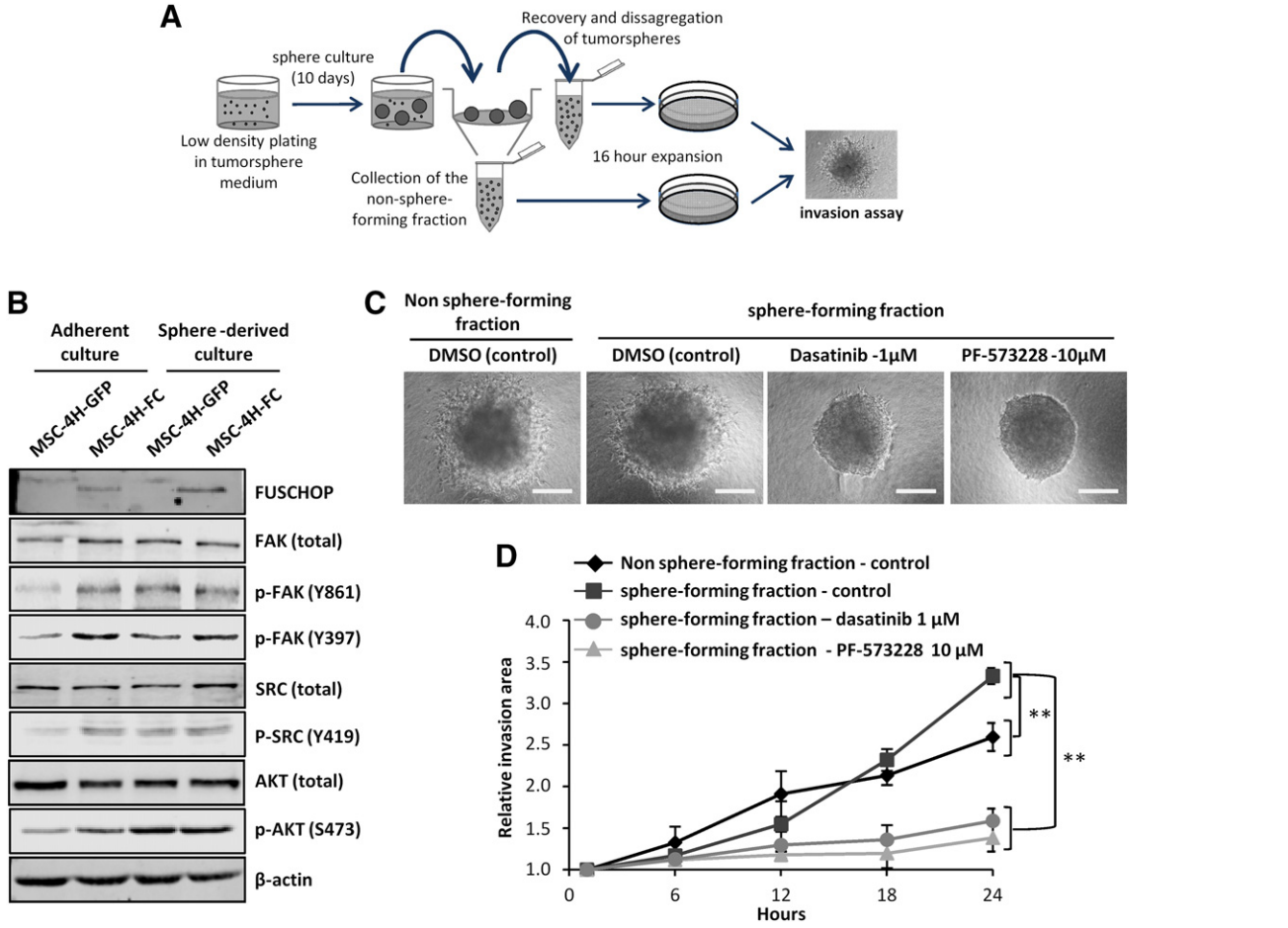

Figure 6. Inhibition of SRC or FAK activation prevents the invasion of CSC-enriched subpopulations. (A) MSC-4H-FC cells were plated at low density in tumorsphere medium and let to form tumorspheres for 10 days. Thereafter, tumorspheres and non–tumorsphere-forming cells were separated and collected. Tumorspheres were disaggregated, and both fractions were allowed to expand to discard nonviable cells before proceeding with the invasion assays. (B) Protein levels of the indicated proteins in adherent cultures or tumorsphere cultures of MSC-4H-FC cells allowed to expand in adherence for 16 hours. Quantification is plotted in Supplementary Fig S6. (C and D) Effect of dasatinib or PF-573228 on the invasive properties of CSC-enriched subpopulations. Representative images of the 3D spheroids of the non–sphere-forming *versus* sphere-forming fractions treated or not with the indicated concentrations of dasatinib or PF-573228 for 24 hours (C) and quantification of the invasive area (D) are presented. Error bars represent the SD, and asterisks indicate statistically significant differences with the control series (**: $P < .01$; one-sided Student *t* test).

cancer cell extravasation *in vivo* in the CAM of chicken embryos. We found that the expression of FUS-CHOP induced the activation of SRC and the upregulation/activation of FAK and enhanced invasive potential. Moreover, using dasatinib, the specific FAK inhibitor PF-573228, and FAK siRNA, we confirmed the hypothesis that the activation of SRC/FAK pathway is mediating the invasive properties induced by FUS-CHOP. Importantly, we show that the inhibition of SRC/FAK is also able to block the invasive potential of CSC subpopulations. Treatment with dasatinib or PF-573228 also had a partial impact on cell proliferation/survival, although these antiproliferative effects become relevant at later time points and/or higher drug concentrations than those that efficiently blocked cell invasion, thus suggesting that these drugs behave as genuine anti-invasive agents in sarcoma cells.

SRC inhibition was able to prevent activating phosphorylation of FAK. However, FAK inhibition did not impede SRC activation. Given that the inhibition of both kinases efficiently inhibits invasion, these findings show that FAK is a downstream effector of SRC activation and its activation is critical for FUS-CHOP–induced invasive phenotype. In accordance with this prominent role of FAK, we found that its expression in sarcoma patient samples significantly correlated with tumor grade and aggressiveness. These findings about the role of FAK in invasion and metastasis are in line with previous studies in other sarcoma subtypes [31,32].

In cancer cells, SRC/FAK pathway activation may induce different types of invasion with different requirements of Rho GTPases [9,12,14,19,20]. We found that FUS-CHOP expression induced an SRC/FAK/RHO/ROCK-dependent accumulation of phospho-MLC2 (T18/S19) which was essential to invade collagen matrices and extravasate out of the CAM vasculature. In line with a preponderant role of RHO/ROCK signaling in the ability of sarcomas to invade, the inhibition of this signaling pathway by different mechanisms was found to prevent invasion in osteosarcoma and Ewing sarcoma [47–50]. It is well established that RHO/ROCK signaling drives the amoeboid type of migration [12,20]. However, it is also known that certain RHO/ROCK activity is required for the contractile activity of actomyosin scaffold to retract the cell rear during the mesenchymal movement [12,51,52]. Historically,

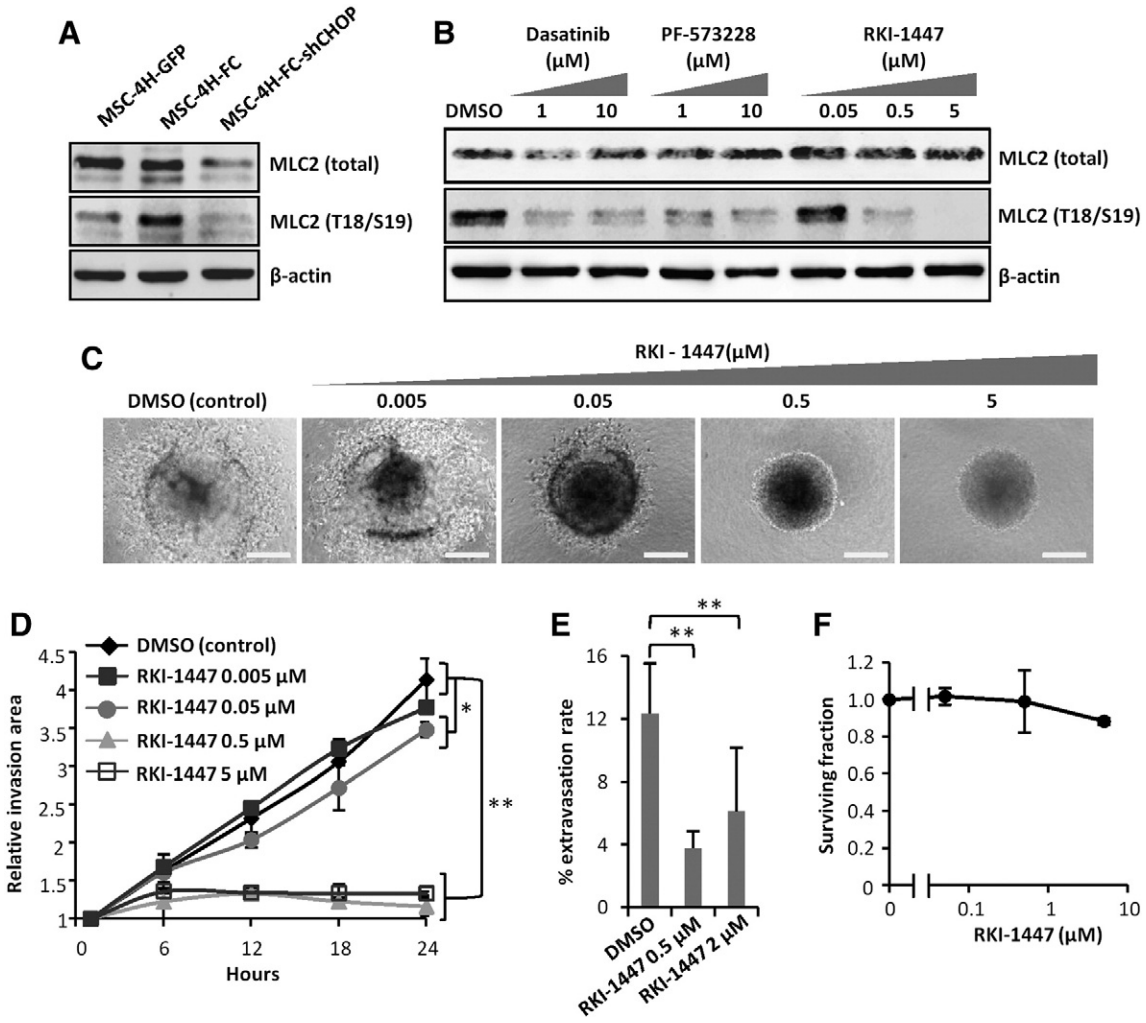

Figure 7. Inhibition of RHO/ROCK signaling prevents the invasion of FUS-CHOP–expressing cells. (A) Western blotting analysis of the indicated proteins in MSC-4H-GFP, MSC-4H-FC, and MSC-4H-FC-shCHOP cells. (B) Western blotting analysis of the indicated proteins in MSC-4H-FC cells treated with increasing concentrations of dasatinib, PF-573228, or RKI-1447 for 24 hours. β-Actin levels were used as loading control. Quantification of three independent experiments is plotted in Supplementary Fig S7. (C and D) Effect of increasing concentrations of RKI-1447 on the invasive properties of MSC-4H-FC cells using 3D spheroid invasion assays. Representative images of the 3D invading spheroids treated with the indicated concentrations of dasatinib for 24 hours (C) and quantification of the invasive area (D) are presented. Scale bars = 200 μm. (E) Quantification of extravasation efficiency of control (DMSO) and RKI-1447 pretreated MSC-4H-FC cells 24 hours postinjection into the chicken embryo CAM vasculature. (F) Cell viability (WST1 assay) measured after the treatment of MSC-4H-FC cells with increasing concentrations of RKI-1447 for 24 hours. Error bars represent the SD, and asterisks indicate statistically significant differences with the control series (*: $P < .05$; **: $P < .01$; one-sided Student t test).

sarcoma cells, which are of mesenchymal origin, were expected to migrate/invade using an elongated/mesenchymal movement [14]. Nevertheless, a RHO-ROCK-dependent amoeboid mode of invasion has also been described as a primary invading mechanism for a model of rat sarcoma cells [53]. In addition, another work showed that HT1080 fibrosarcoma cells embedded as spheroids in 3D collagen matrices displayed a transition in morphology from round to elongated as a function of increasing radial position into the spheroid. Interestingly, in this collective invasion model, cells presenting elongated-mesenchymal morphology at the periphery of the spheroids migrated faster, and their dissemination into the surrounding matrix was dependent on ROCK/MLC2-driven contractility [21]. In line with these findings, cells at the periphery of the MRCLS spheroids displayed an elongated morphology in the 3D invasion assays herein described, and their mode of invasion was found to be dependent on RHO/ROCK activity. These data suggest that intermediate situations may exist between mesenchymal and amoeboid models of invasion which may depend on specific cell determinants and environmental conditions [16,46].

Conclusions

The herein presented data uncover a novel mechanism by which the fusion oncogene FUS-CHOP actively promotes invasion in myxoid and round cell liposarcoma through the activation of a SRC/FAK/RHO/ROCK signaling axis. In addition, we found that FAK expression significantly correlates with tumor aggressiveness and advanced disease stage in sarcoma patient samples. Therefore, the inhibition of this signaling could represent a potential antimetastatic therapeutic strategy for this type of tumors.

Supplementary data to this article can be found online at https://doi.org/10.1016/j.neo.2017.11.004.

Conflict of Interest Disclosure Statement

The authors declare no competing financial interests.

Funding

This work was supported by the Agencia Estatal de Investigación (AEI) [MINECO/Fondo Europeo de Desarrollo Regional (FEDER) (SAF-2013-42,946-R and SAF-2016-75,286-R to R.R.), ISC III/FEDER (Miguel Servet II Program CPII16/00049 to R.R. and PI13/00259 and PI16/00280 to J.M.G-P) and Consorcio CIBERONC CB16/12/00390 to J.P.R)] and the Plan de Ciencia Tecnología e Innovación del Principado de Asturias (GRUPIN14-003) to J. P. R. H. S. L. is supported by Prostate Cancer Canada Rising Star Grant (RS2016-1011).

References

[1] De Vita A, Mercatali L, Recine F, Pieri F, Riva N, Bongiovanni A, Liverani C, Spadazzi C, Miserocchi G, and Amadori D, et al (2016). Current classification, treatment options, and new perspectives in the management of adipocytic sarcomas. *Onco Targets Ther* **9**, 6233–6246.

[2] Patil N, Ahmed Kabeer Rasheed S, Abba M, Hendrik Leupold J, Schwarzbach M, and Allgayer H (2014). A mechanistic study on the metastasis inducing function of FUS-CHOP fusion protein in liposarcoma. *Int J Cancer* **134**, 2808–2819.

[3] Martinez-Cruzado L, Tornin J, Rodriguez A, Santos L, Allonca E, Fernandez-Garcia MT, Astudillo A, Garcia-Pedrero JM, and Rodriguez R (2017). Trabectedin and campthotecin synergistically eliminate cancer stem cells in cell-of-origin sarcoma models. *Neoplasia* **19**, 460–470.

[4] McLean GW, Carragher NO, Avizienyte E, Evans J, Brunton VG, and Frame MC (2005). The role of focal-adhesion kinase in cancer—a new therapeutic opportunity. *Nat Rev Cancer* **5**, 505–515.

[5] Mitra SK and Schlaepfer DD (2006). Integrin-regulated FAK-Src signaling in normal and cancer cells. *Curr Opin Cell Biol* **18**, 516–523.

[6] Playford MP and Schaller MD (2004). The interplay between Src and integrins in normal and tumor biology. *Oncogene* **23**, 7928–7946.

[7] Roskoski Jr R (2015). Src protein-tyrosine kinase structure, mechanism, and small molecule inhibitors. *Pharmacol Res* **94**, 9–25.

[8] Amata I, Maffei M, and Pons M (2014). Phosphorylation of unique domains of Src family kinases. *Front Genet* **5**, 1–6, 181.

[9] Guarino M (2010). Src signaling in cancer invasion. *J Cell Physiol* **223**, 14–26.

[10] Huveneers S and Danen EH (2009). Adhesion signaling—crosstalk between integrins, Src and Rho. *J Cell Sci* **122**, 1059–1069.

[11] Canel M, Secades P, Garzon-Arango M, Allonca E, Suarez C, Serrels A, Frame M, Brunton V, and Chiara MD (2008). Involvement of focal adhesion kinase in cellular invasion of head and neck squamous cell carcinomas via regulation of MMP-2 expression. *Br J Cancer* **98**, 1274–1284.

[12] Pandya P, Orgaz JL, and Sanz-Moreno V (2017). Modes of invasion during tumour dissemination. *Mol Oncol* **11**, 5–27.

[13] Struckhoff AP, Rana MK, and Worthylake RA (2011). RhoA can lead the way in tumor cell invasion and metastasis. *Front Biosci (Landmark Ed)* **16**, 1915–1926.

[14] Wolf K and Friedl P (2006). Molecular mechanisms of cancer cell invasion and plasticity. *Br J Dermatol* **154**(Suppl. 1), 11–15.

[15] Zhu L, McManus MM, and Hughes DP (2013). Understanding the biology of bone sarcoma from early initiating events through late events in metastasis and disease progression. *Front Oncol* **3**, 1–17, 230.

[16] Clark AG and Vignjevic DM (2015). Modes of cancer cell invasion and the role of the microenvironment. *Curr Opin Cell Biol* **36**, 13–22.

[17] Friedl P, Locker J, Sahai E, and Segall JE (2012). Classifying collective cancer cell invasion. *Nat Cell Biol* **14**, 777–783.

[18] Friedl P and Alexander S (2011). Cancer invasion and the microenvironment: plasticity and reciprocity. *Cell* **147**, 992–1009.

[19] Sahai E and Marshall CJ (2003). Differing modes of tumour cell invasion have distinct requirements for Rho/ROCK signalling and extracellular proteolysis. *Nat Cell Biol* **5**, 711–719.

[20] Yamazaki D, Kurisu S, and Takenawa T (2009). Involvement of Rac and Rho signaling in cancer cell motility in 3D substrates. *Oncogene* **28**, 1570–1583.

[21] Jimenez Valencia AM, Wu PH, Yogurtcu ON, Rao P, DiGiacomo J, Godet I, He L, Lee MH, Gilkes D, and Sun SX, et al (2015). Collective cancer cell invasion induced by coordinated contractile stresses. *Oncotarget* **6**, 43438–43451.

[22] Canel M, Secades P, Rodrigo JP, Cabanillas R, Herrero A, Suarez C, and Chiara MD (2006). Overexpression of focal adhesion kinase in head and neck squamous cell carcinoma is independent of fak gene copy number. *Clin Cancer Res* **12**, 3272–3279.

[23] Orgaz JL, Herraiz C, and Sanz-Moreno V (2014). Rho GTPases modulate malignant transformation of tumor cells. *Small GTPases* **5**, 1–15, e29019.

[24] Rodrigo JP, Alvarez-Alija G, Menendez ST, Mancebo G, Allonca E, Garcia-Carracedo D, Fresno MF, Suarez C, and Garcia-Pedrero JM (2011). Cortactin and focal adhesion kinase as predictors of cancer risk in patients with laryngeal premalignancy. *Cancer Prev Res (Phila)* **4**, 1333–1341.

[25] Vlaeminck-Guillem V, Gillet G, and Rimokh R (2014). SRC: marker or actor in prostate cancer aggressiveness. *Front Oncol* **4**, 222.

[26] Montero JC, Seoane S, Ocana A, and Pandiella A (2011). Inhibition of SRC family kinases and receptor tyrosine kinases by dasatinib: possible combinations in solid tumors. *Clin Cancer Res* **17**, 5546–5552.

[27] Shanthi E, Krishna MH, Arunesh GM, Venkateswara Reddy K, Sooriya Kumar J, and Viswanadhan VN (2014). Focal adhesion kinase inhibitors in the treatment of metastatic cancer: a patent review. *Expert Opin Ther Pat* **24**, 1077–1100.

[28] Michels S, Trautmann M, Sievers E, Kindler D, Huss S, Renner M, Friedrichs N, Kirfel J, Steiner S, and Endl E, et al (2013). SRC signaling is crucial in the growth of synovial sarcoma cells. *Cancer Res* **73**, 2518–2528.

[29] Sievers E, Trautmann M, Kindler D, Huss S, Gruenewald I, Dirksen U, Renner M, Mechtersheimer G, Pedeutour F, and Aman P, et al (2015). SRC inhibition represents a potential therapeutic strategy in liposarcoma. *Int J Cancer* **137**, 2578–2588.

[30] Shor AC, Keschman EA, Lee FY, Muro-Cacho C, Letson GD, Trent JC, Pledger WJ, and Jove R (2007). Dasatinib inhibits migration and invasion in diverse human sarcoma cell lines and induces apoptosis in bone sarcoma cells dependent on SRC kinase for survival. *Cancer Res* **67**, 2800–2808.

[31] Ren K, Lu X, Yao N, Chen Y, Yang A, Chen H, Zhang J, Wu S, Shi X, and Wang C, et al (2015). Focal adhesion kinase overexpression and its impact on human osteosarcoma. *Oncotarget* **6**, 31085–31103.

[32] Waters AM, Stafman LL, Garner EF, Mruthyunjayappa S, Stewart JE, Mroczek-Musulman E, and Beierle EA (2016). Targeting focal adhesion kinase suppresses the malignant phenotype in rhabdomyosarcoma cells. *Transl Oncol* **9**, 263–273.

[33] Rodriguez R, Tornin J, Suarez C, Astudillo A, Rubio R, Yauk C, Williams A, Rosu-Myles M, Funes JM, and Boshoff C, et al (2013). Expression of FUS-CHOP fusion protein in immortalized/transformed human mesenchymal stem cells drives mixoid liposarcoma formation. *Stem Cells* **31**, 2061–2072.

[34] Funes JM, Quintero M, Henderson S, Martinez D, Qureshi U, Westwood C, Clements MO, Bourboulia D, Pedley RB, and Moncada S, et al (2007). Transformation of human mesenchymal stem cells increases their dependency on oxidative phosphorylation for energy production. *Proc Natl Acad Sci U S A* **104**, 6223–6228.

[35] Rodriguez R, Rosu-Myles M, Arauzo-Bravo M, Horrillo A, Pan Q, Gonzalez-Rey E, Delgado M, and Menendez P (2014). Human bone marrow stromal cells lose immunosuppressive and anti-inflammatory properties upon oncogenic transformation. *Stem Cell Rep* **3**, 606–619.

[36] Tornin J, Martinez-Cruzado L, Santos L, Rodriguez A, Nunez LE, Oro P, Hermosilla MA, Allonca E, Fernandez-Garcia MT, and Astudillo A, et al (2016). Inhibition of SP1 by the mithramycin analog EC-8042 efficiently targets tumor initiating cells in sarcoma. *Oncotarget* **7**, 30935–30950.

[37] Coindre JM, Trojani M, Contesso G, David M, Rouesse J, Bui NB, Bodaert A, De Mascarel I, De Mascarel A, and Goussot JF (1986). Reproducibility of a histopathologic grading system for adult soft tissue sarcoma. *Cancer* **58**, 306–309.

[38] Kim Y, Williams KC, Gavin CT, Jardine E, Chambers AF, and Leong HS (2016). Quantification of cancer cell extravasation in vivo. *Nat Protoc* **11**, 937–948.

[39] Abarrategi A, Tornin J, Martinez-Cruzado L, Hamilton A, Martinez-Campos E, Rodrigo JP, Gonzalez MV, Baldini N, Garcia-Castro J, and Rodriguez R (2016).

Osteosarcoma: cells-of-origin, cancer stem cells, and targeted therapies. *Stem Cells Int* **2016**, 1–13, 3631764.

[40] Rodriguez R, Rubio R, and Menendez P (2012). Modeling sarcomagenesis using multipotent mesenchymal stem cells. *Cell Res* **22**, 62–77.

[41] Willems SM, Schrage YM, Bruijn IH, Szuhai K, Hogendoorn PC, and Bovee JV (2010). Kinome profiling of myxoid liposarcoma reveals NF-kappaB-pathway kinase activity and casein kinase II inhibition as a potential treatment option. *Mol Cancer* **9**, 1–12, 257.

[42] Smalley KS, Lioni M, Noma K, Haass NK, and Herlyn M (2008). In vitro three-dimensional tumor microenvironment models for anticancer drug discovery. *Expert Opin Drug Discov* **3**, 1–10.

[43] Leong HS, Robertson AE, Stoletov K, Leith SJ, Chin CA, Chien AE, Hague MN, Ablack A, Carmine-Simmen K, and McPherson VA, et al (2014). Invadopodia are required for cancer cell extravasation and are a therapeutic target for metastasis. *Cell Rep* **8**, 1558–1570.

[44] Martinez-Cruzado L, Tornin J, Santos L, Rodriguez A, Garcia-Castro J, Moris F, and Rodriguez R (2016). Aldh1 expression and activity increase during tumor evolution in sarcoma cancer stem cell populations. *Sci Rep* **6**, 1–14, 27878.

[45] Patel RA, Forinash KD, Pireddu R, Sun Y, Sun N, Martin MP, Schonbrunn E, Lawrence NJ, and Sebti SM (2012). RKI-1447 is a potent inhibitor of the Rho-associated ROCK kinases with anti-invasive and antitumor activities in breast cancer. *Cancer Res* **72**, 5025–5034.

[46] Wolf K and Friedl P (2011). Extracellular matrix determinants of proteolytic and non-proteolytic cell migration. *Trends Cell Biol* **21**, 736–744.

[47] Kosla J, Pankova D, Plachy J, Tolde O, Bicanova K, Dvorak M, Rosel D, and Brabek J (2013). Metastasis of aggressive amoeboid sarcoma cells is dependent on Rho/ROCK/MLC signaling. *Cell Commun Signal* **11**, 1–13, 51.

[48] Pinca RS, Manara MC, Chiadini V, Picci P, Zucchini C, and Scotlandi K (2017). Targeting ROCK2 rather than ROCK1 inhibits Ewing sarcoma malignancy. *Oncol Rep* **37**, 1387–1393.

[49] Wang W, Zhou X, and Wei M (2015). MicroRNA-144 suppresses osteosarcoma growth and metastasis by targeting ROCK1 and ROCK2. *Oncotarget* **6**, 10297–10308.

[50] Wang Y, Zhao W, and Fu Q (2013). miR-335 suppresses migration and invasion by targeting ROCK1 in osteosarcoma cells. *Mol Cell Biochem* **384**, 105–111.

[51] Friedl P and Wolf K (2009). Proteolytic interstitial cell migration: a five-step process. *Cancer Metastasis Rev* **28**, 129–135.

[52] Ridley AJ, Schwartz MA, Burridge K, Firtel RA, Ginsberg MH, Borisy G, Parsons JT, and Horwitz AR (2003). Cell migration: integrating signals from front to back. *Science* **302**, 1704–1709.

[53] Rosel D, Brabek J, Tolde O, Mierke CT, Zitterbart DP, Raupach C, Bicanova K, Kollmannsberger P, Pankova D, and Vesely P, et al (2008). Up-regulation of Rho/ROCK signaling in sarcoma cells drives invasion and increased generation of protrusive forces. *Mol Cancer Res* **6**, 1410–1420.